International Conference on Non-conventional Materials and Technologies
NOCMAT 2022

FINITE ELEMENT ANALYSIS FOR THE PREDICTION OF THE CIRCUMFERENTIAL BAMBOO STRENGTH

Silvia Greco, DICAM - Università di Bologna, Italy, s.greco@unibo.it
Luisa Molari, DICAM - Università di Bologna, Italy, luisa.molari@unibo.it
Giovanni Valdrè, BIGEA - Università di Bologna, Italy, giovanni.valdre@unibo.it
Jose Jaime Garcia, Escuela de Ingeniería Civil y Geomática - Universidad del Valle, Colombia, jose.garcia@correounivalle.edu.co

ABSTRACT

Reported theoretical analyses have not explained the variation with radius of the circumferential strength of bamboo. This study aims to analyze this issue using finite element analysis. A rectangular image representative of the culm cross section of *Phyllostachys edulis* was divided along the radial direction into ten parts. Next, ten FE rectangular models representing the fibers, matrix, and void content at each radial position were generated. The matrix and the fibers were assumed to be isotropic, having elastic moduli of 1800 MPa and 18000 MPa, respectively. The strength predicted with the fiber first principal stress is parabolic along the radial direction, consistent with experimental findings.

KEYWORDS

Bamboo strength; bamboo radial gradation; bamboo finite element analysis

INTRODUCTION

Locally sourced natural materials like bamboo represent a viable alternative for sustainable construction. Bamboo combines high mechanical resistance with a low specific weight and a very high growth speed, becoming able to provide material to replace timber in the coming future. Advancement in the application of bamboo in the modern era requires further understanding of the material properties, anatomy, and strength at different locations and positions in the bamboo culms (Wahab et al., 2012).

Bamboo has a heterogeneous section (Grosser & Liese, 1971) composed of voids, fibres, and parenchyma, which play different roles in the mechanical performance of the material. Fibres are cells with a strongly thickened secondary wall subjected to lignification, which provides strength and stiffness to the culm. Fibres are grouped into bundles that are clearly visible in the section of the plant, and their amount and dimension change significantly. Parenchyma cells are elongated and not prone to lignification, which acts as a matrix along the complete length of the fibers. Voids are nourishing substance distribution tubes that can change significantly depending on the plant's position and age (Li et al., 2007).

Mechanical properties of bamboo components have been measured in many studies (Amada et al., 1996; Shao et al., 2010; Habibi et al., 2015) with different methods, leading to very different results (Akinbade & Harries, 2021), which have been collected in existing literature for P. edulis. For example, the fibre longitudinal modulus of elasticity is in the range of 5.9 to 55 GPa, while the matrix longitudinal modulus of elasticity is between 0.2 and 5.8 GPa. The Rule of Mixture (ROM) is widely used to calculate the properties of fiber-reinforced composite materials. It works well in longitudinal applications, while in transversal ones, the Halpin-Tsai correction is usually needed. The use of the ROM in the transversal direction is controversial (Akinbade & Harries, 2021), particularly, when used to describe the variation

with radius of the circumferential strength obtained in experiments. Thus, in this paper, a pilot finite element analysis is presented to analyse the circumferential strength of the material at different radial positions along the culm wall.

METHODS

The microscopic images (Figure 1a) were obtained with polarized optical microscopy (POM) by using thin sections (about 30 ± 1 µm), polished to at least 0.5 µm. Both reflected and transmission polarized optical microscopy analyses were performed on the thin sections employing a Zeiss Photomicroscope III with polarized light and digitized with an Edmund Optics CMOS-sensor. Then, the microscopical image of bamboo (Figure 1a) was used to create 10 models representing the content and form of the matrix, fibers, and voids along the radial direction.

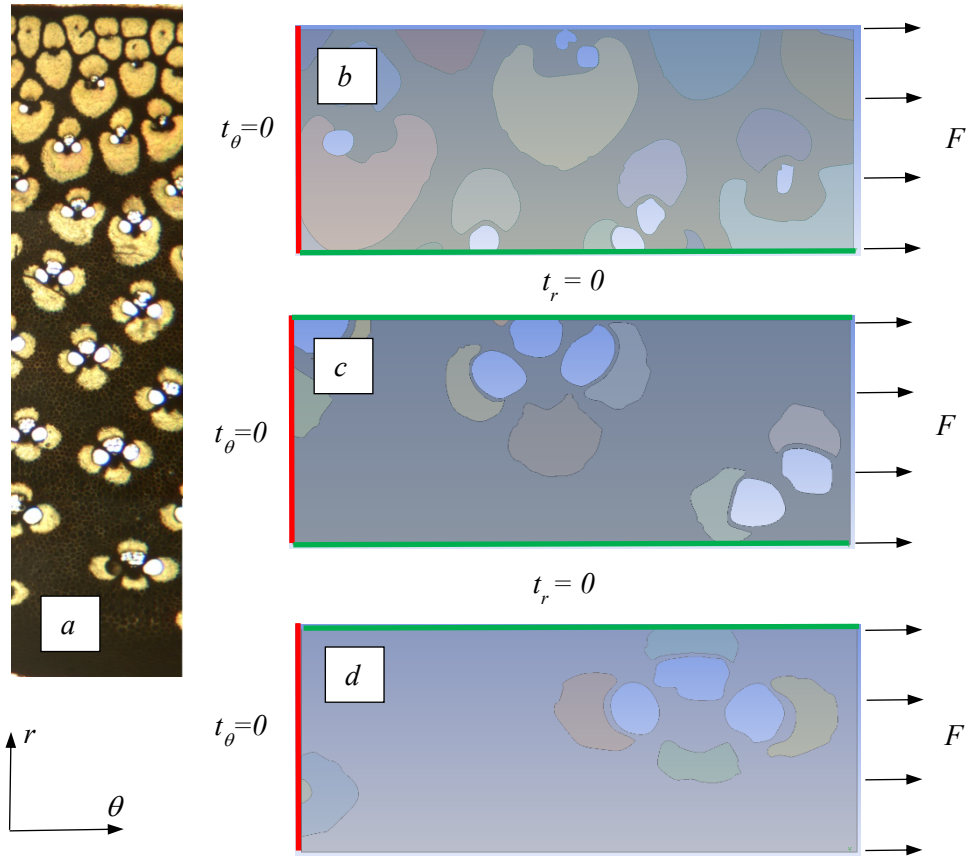

Figure 1. *a*. Image considered, and geometry of the models at radial positions equal to *b*. 0.85, *c.* 0.5, and *d.* 0.15, normalized over the wall thickness. The tangential displacement t_θ was restrained on the red lines, whereas the radial displacement t_r on the green lines

The geometry of each model was accomplished in the student version of the pre-post processor GID (https://www.gidhome.com/). First, a .dxf version of the image was imported into GID (Figure 1). This image is composed of points and lines representing the contours between the contents. The line contours were then used to generate the areas representative of the fibres and the matrix, while no area was created in the contours defining the voids. Next, the image was divided into 10 parts of the same height (*w)* measured along the radial direction. Each portion of the image was used to create the geometry of the finite element model, representative of the microstructure of the material at every radial position.

The following step consisted of importing each of these geometrical models into the program Ansys (www.ansys.com). In this program, a plain strain model was considered since the material is restricted to deforming along the longitudinal direction of the culm, i.e. perpendicular to the image. The circumferential displacements were fixed on the left boundary, and a uniformly distributed circumferential force was prescribed for the right boundary. Consistent with the restriction of the material adjacent to the models, the radial displacement t_r was also prescribed on the lower face of the model of the outer part of the wall (Figure 1.b), both faces of the eight models in the middle (Figure 2.c), and the upper face of the model of the inner part of the wall (Figure 2.d). It was assumed that there was a perfect bond between the matrix and the fibers. The elastic moduli of the constituents were assumed to be 1800 MPa and 18000 MPa for the matrix and fibers, respectively [1].

The goal of the analyses in terms of strength was to determine the variation of circumferential stress along the radial direction for the assessment of strength at one position relative to the others. Thus, it was assumed that the mechanical properties of the fibers and the matrix did not change with radial position. The principal stress as well as the Von Mises components were analysed. Thus, the maximum values of the first principal and maximum Von Mises components were recorded at each radial position. The strength was considered to be higher for those sections displaying lower values of the stress components. If the ultimate stress of the fibers and matrix were known, the equation needed to check the resistance would be,

$$s_{imax} \leq S_u; \qquad \frac{s_{imax}}{S_u} \leq 1; \qquad 0 \leq 1 - \frac{s_{imax}}{S_u} \tag{1}$$

where s_{imax} is the maximum value of the stress component (either first principal or Von Mises) at the radial position i. As the strength of the fibers and matrix is unknown, the relative strength at each position was estimated by replacing S_u by the maximum stress S_{max} recorded in the 10 models. Thus, the strength index I_{si} for each position *i* was defined as follows,

$$I_{si} = 1 - \frac{s_{imax}}{S_{max}}. \tag{2}$$

In other words, I_{si} indicates how far the stress is at each position from the maximum. Second-order polynomial fittings were performed for I_{si}, which were calculated for the matrix and the fibers. As the models include geometrical nonlinearities, two levels of force were considered, equal to 250 N and 40 N.

RESULTS

The contours of the first principal stress component show concentrations in the fibers around the voids (Figure 2). The correlation coefficient for the parabolic interpolation of the stress index along the radial direction shows the best values for the first principal stress in the fibers (Figure 3, Table 2) and poor values for the Von Mises stress in the fibers and in the matrix. A relatively small variation was obtained for the stress index with respect to load level.

Table 2. Coefficient of determination R^2 for the strength index considering the first principal stress in the matrix S_m, and in the fibers S_f; and the Von Mises stress in the matrix VM_m, and in the fibers VM_f. Two load levels were analyzed.

	S_m	S_f	VM_m	VM_f
40 N	0.34	0.69	0.24	0.39
250 N	0.33	0.67	0.28	0.23

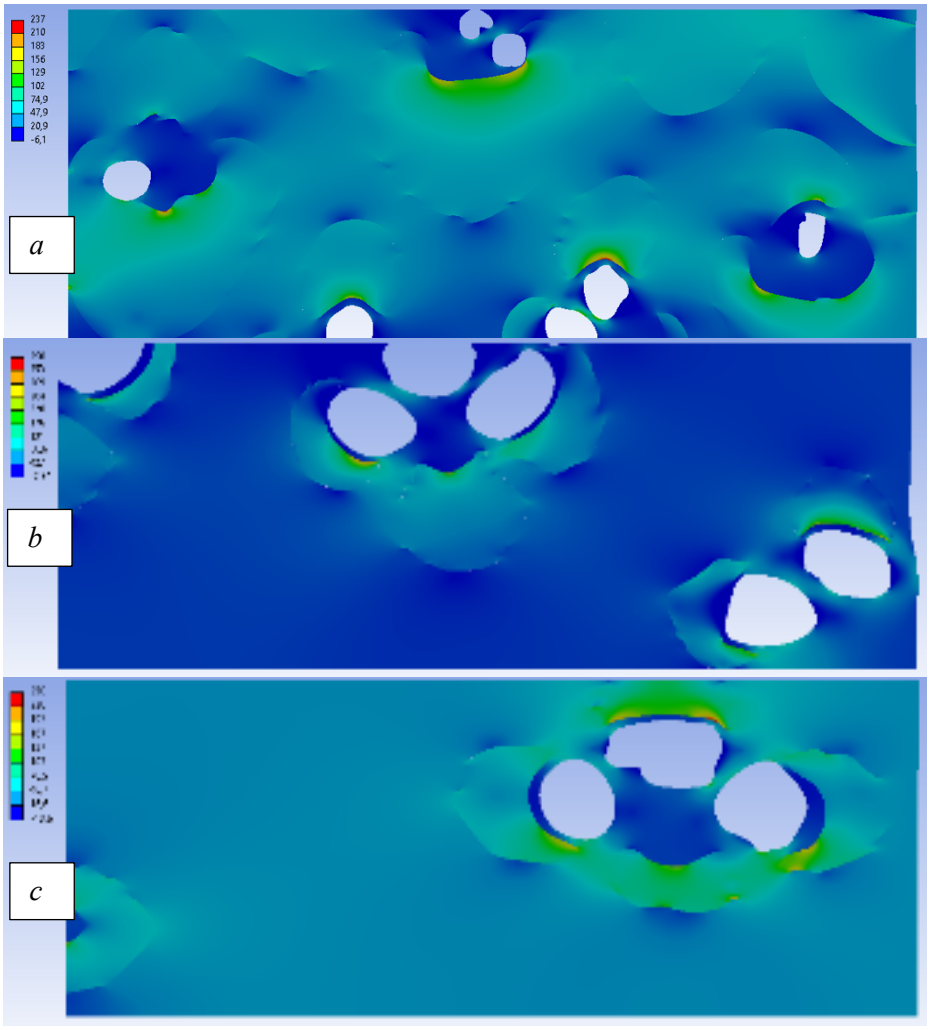

Figure 3. First principal stress contours in the models at normalized radial positions of *a*. 0.85, *b.* 0.5, *c*. 0.15. Stress concentrations are developed around the voids.

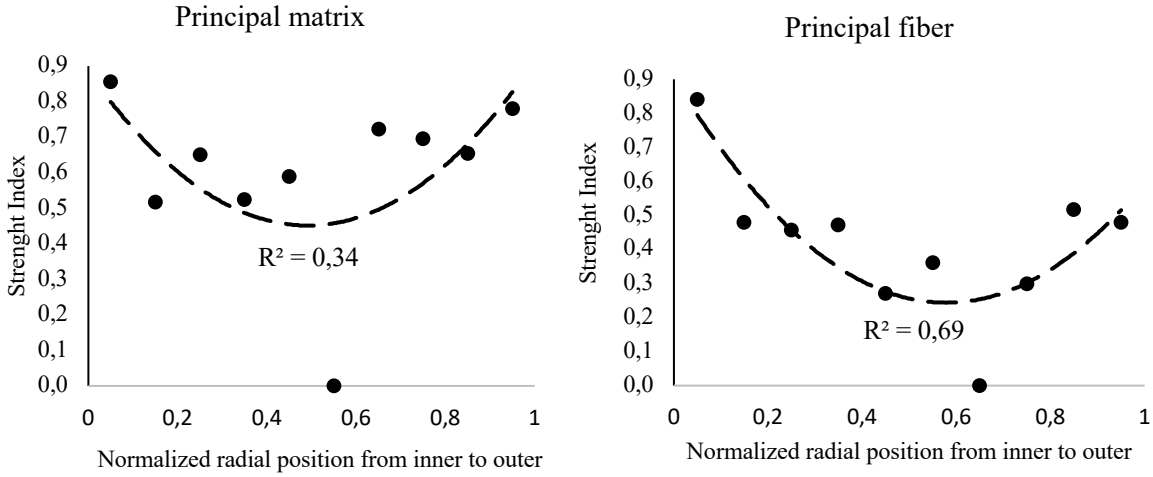

Figure 4. Variation of the strength index along the radial direction considering the first principal stress in the matrix (left) and in the fibers (right).

DISCUSSION

Results of the finite element analysis show that the first principal stress in the fibers is the better predictor of a parabolic variation of strength along the circumferential direction, consistent with experimental findings (Akinbade & Harries, 2021). In contrast, the Von Mises stress component does predict a poor parabolic correlation. These two results are consistent with the brittle behavior of the material, since the Von Mises criterion is valid for ductile materials. More analyses have to be accomplished to validate these initial findings.

CONCLUSIONS

1. Finite element models taking into account the microstructure of bamboo may be a feasible alternative to analyze relative variations of strength with position.
2. As the strength of the matrix and the fibers was assumed to be constant along the radial direction, the predicted parabolic variation of strength along the radial direction may be attributed to changes in the stress concentration factors.
3. The stress concentrators depend to a high extent on the density and position of the voids, that are surrounded by the fibers, thus creating high stress in their transverse plane. In this sense, the vessels modeled as holes increase the stress concentrations.

REFERENCE

Akinbade, Y., & Harries, K. (2021). Is the rule of mixture appropriate for assessing bamboo material properties? *Construction and Building Materials, 267* https://doi.org/10.1016/j.conbuildmat.2020.120955

Amada, S., Munekata, T., Nagase, Y., Ichikawa, Y., Kirigai, A., & Zhifei, Y. (1996). The Mechanical Structures of Bamboos in Viewpoint of Functionally Graded and Composite Material. *Journal of Composite Materials, 30*(7), 800-819. doi:0021-9983/96/07 800-20

Grosser, D., & Liese, W. (1971). On the Anatomy of Asian Bamboos, with Special Reference to their Vascular Bundles. *Wood Science and Technology, 5*, 290-312.

K.Habibi, M., T.Samaei, A., Gheshlaghi, B., Lu, J., & Lu, Y. (2015). Asymmetric flexural behavior from bamboo's functionally graded hierarchical structure: Underlying mechanisms. *Acta Biomateralia, 16*, 178-186. https://doi.org/10.1016/j.actbio.2015.01.038

Li, X., Shupe, T., Peter, G., Hse, C., & Eberhardt, T. (2007). Chemical changes with maturation of the bamboo species phyllostachys pubescens. *Journal of Tropical Forest Science, 19*(1), 6-12.

Shao, Z.-P., Fang, C.-H., Huang, S.-X., & Tian, G.-L. (2010). Tensile properties of Moso bamboo (Phyllostachys pubescens) and its components with respect to its fiber-reinforced composite structure. *Wood Science and Technology, 44*, 655-666. https://doi.org/10.1007/s00226-009-0290-1

Wahab, R., Mustafa, M. T., Rahman, S., Salam, M. A., Sulaiman, O., Sudin, M., & Rasat, M. S. (2012). Relationship between physical, anatomical and strenght properties of a 3-year-old cultivated tropical bamboo. *ARPN Journal of Agricultural and Biological Science, 7*(10), 782-791. doi:ISSN 1990-6145

ACKNOWLEDGEMENT

J.J. García acknowledges the financial support provided by a research grant (No. 21131) from the Universidad del Valle (Colombia), as part of the project "Advanced models to characterize the viscoelasticity of *Guadua* in the transverse plane".

CONFLICT OF INTEREST

The authors declare that they have no conflicts of interest associated with the work presented in this paper.

DATA AVAILABILITY

Data on which this paper is based is available from the authors upon reasonable request.